

An epigenetic mechanism for cavefish eye degeneration

Aniket V. Gore¹✉, Kelly A. Tomins¹, James Iben², Li Ma³, Daniel Castranova¹, Andrew E. Davis¹, Amy Parkhurst¹, William R. Jeffery³ and Brant M. Weinstein¹✉

Coding and non-coding mutations in DNA contribute significantly to phenotypic variability during evolution. However, less is known about the role of epigenetics in this process. Although previous studies have identified eye development genes associated with the loss-of-eyes phenotype in the Pachón blind cave morph of the Mexican tetra *Astyanax mexicanus*, no inactivating mutations have been found in any of these genes. Here, we show that excess DNA methylation-based epigenetic silencing promotes eye degeneration in blind cave *A. mexicanus*. By performing parallel analyses in *A. mexicanus* cave and surface morphs, and in the zebrafish *Danio rerio*, we have discovered that DNA methylation mediates eye-specific gene repression and globally regulates early eye development. The most significantly hypermethylated and downregulated genes in the cave morph are also linked to human eye disorders, suggesting that the function of these genes is conserved across vertebrates. Our results show that changes in DNA methylation-based gene repression can serve as an important molecular mechanism generating phenotypic diversity during development and evolution.

Subterranean animals offer an excellent opportunity to study morphological, molecular and physiological changes that allow organisms to adapt to unique environments. Loss of eyes is one of the most common morphological features of cave-adapted animals, including many fish species. Blind cave morphs of *Astyanax mexicanus* evolved from surface fish during a few million years of isolation in dark Mexican caves¹, with recent studies suggesting that regression of the eyes evolved as part of a strategy to conserve energy in fish adapted to dark and nutrient-deficient caves². Although a number of studies have examined molecular mechanisms underlying eye loss in Pachón cave-derived *A. mexicanus* cavefish, recent sequencing of the Pachón cavefish genome and other studies revealed no inactivating null mutations in essential eye development genes^{3–7}. In contrast, genome sequencing of another subterranean animal—the naked mole rat *Heterocephalus glaber*—showed combined functional loss of more than a dozen key eye genes due to inactivating mutations⁸. The absence of obvious null mutations in essential eye genes despite dramatic effects on eye development suggests the possibility that Pachón cavefish might harbour *cis*-regulatory mutations causing altered expression of eye genes and epigenetic regulators, and most likely the epigenetic regulation indirectly affecting the expression of large numbers of target eye genes at the same time. DNA methylation is one such epigenetic mechanism that is known to be able to simultaneously alter the expression of large cohorts of genes⁹. To test the possibility that altered DNA methylation plays a role in Pachón cavefish eye loss, we used cave and surface fish morphs of *A. mexicanus*, as well as wild-type and DNA methylation and demethylation-deficient zebrafish *Danio rerio*, to examine whether DNA methylation regulates eye formation, and whether eye loss in Pachón cavefish evolved at least in part through hypermethylation of key eye genes.

Results and discussion

At 36 h post-fertilization, *A. mexicanus* cave and surface fish embryos are superficially indistinguishable, with properly formed

lenses and optic cups in both morphs (Fig. 1a,b). However, by five days of development, degeneration of the eye tissue is clearly evident (Fig. 1c,d), and by adulthood, cavefish eyes are completely absent (Fig. 1e,f)¹⁰. Eye regression is preceded by decreased expression of a number of different eye-specific genes, including the crystallins *crybb1*, *crybb1c* and *cryaa* (Fig. 1g). The expression of large sets of genes can be repressed by DNA methylation-based epigenetic silencing, as perhaps most famously shown for X chromosome inactivation¹¹. New epigenetic DNA methyl 'marks' are added by specific enzymes known as de novo DNA methyltransferases (DNMTs)¹², and we recently showed that one of these enzymes, *dnmt3bb.1*, is expressed in zebrafish haematopoietic stem and progenitor cells, where its loss leads to failure to maintain these cells¹³. We found that *dnmt3bb.1* is also expressed in the ciliary marginal zone of the developing eye—a specialized stem-cell-containing tissue surrounding the lens that is responsible for generating neurons and other eye cell types^{14–16} (Fig. 1h). In addition to their haematopoietic defects, *dnmt3bb.1*²⁵⁸ null mutant larvae and adults have enlarged eyes compared with their wild-type siblings (Fig. 1i–k) with retinal hyperplasia (Supplementary Fig. 1), and increased expression of a number of different eye genes, including *opn1lw1*, *gnb3a* and *crx* (Fig. 1l). Interestingly, the closely related *A. mexicanus dnmt3bb.1* gene, which also maps to an eye size quantitative trait locus⁶, shows 1.5-fold increased expression in Pachón cavefish compared with surface fish (Fig. 1m and Supplementary Fig. 2). The inverse correlation between eye size and *dnmt3bb.1* expression in *D. rerio* and *A. mexicanus* led us to hypothesize that excessive Dnmt3bb.1-dependent methylation may globally repress the expression of eye genes in cavefish.

To more comprehensively examine whether increased DNA methylation correlates with reduced eye gene expression in cavefish versus surface fish, we performed combined RNA sequencing (RNA-Seq) and whole-genome bisulphite sequencing on RNA and DNA simultaneously co-isolated from cavefish or surface

¹Division of Developmental Biology, Eunice Kennedy Shriver National Institute of Child Health and Human Development, NIH, Bethesda, MD, USA.

²Molecular Genomics Laboratory, Eunice Kennedy Shriver National Institute of Child Health and Human Development, NIH, Bethesda, MD, USA.

³Department of Biology, University of Maryland, College Park, MD, USA. *e-mail: gore.aniket@nih.gov; bw96w@nih.gov

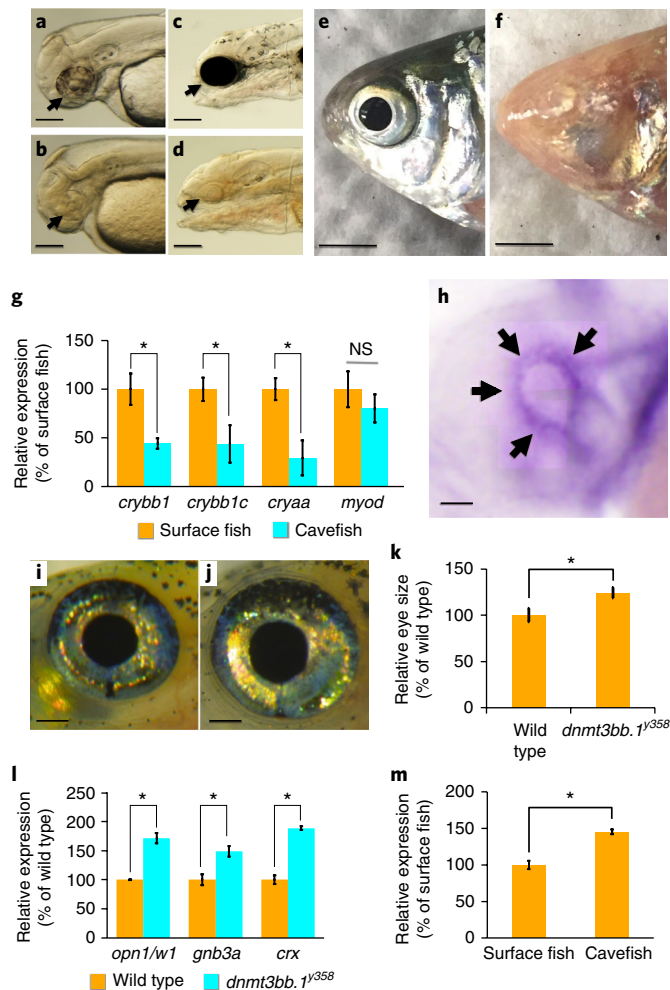


Fig. 1 | Eye phenotypes in *A. mexicanus* surface fish and cavefish, and *D. rerio* wild-type and *dnmt3bb.1*²⁵⁸ mutants. a–d, Transmitted light photomicrographs of the heads of surface (a and c) and cavefish (b and d) morphs of *A. mexicanus* at 36 h post-fertilization (a and b) and 5 days post-fertilization (c and d). Black arrows mark the developing eyes. **e, f**, Photographs of the heads of adult surface (e, with eyes) and cave (f, eyeless) morphs of *A. mexicanus*. **g**, Quantitative RT-PCR analysis of the percentage relative expression of *crybb1*, *crybb1c*, *cryaa* and *myod* in isolated heads from surface (orange columns) and cave (blue columns) morphs of *A. mexicanus* at 54 h post-fertilization, normalized to surface fish levels. Data represent means \pm s.e.m. of three biological replicates (two-tailed *t*-test, $*P < 0.005$). NS, not significant. **h**, Whole-mount in situ hybridization of a zebrafish eye probed for *dnmt3bb.1* at 36 h post-fertilization, showing expression in the ciliary marginal zone (arrows). **i, j**, Photographs of the eyes of adult wild-type sibling (i) and *dnmt3bb.1*²⁵⁸ mutant (j) zebrafish. **k**, Quantitation of eye size in three-week-old wild-type sibling and *dnmt3bb.1*²⁵⁸ mutant zebrafish. Data represent means \pm s.d. ($n = 18$) (two-tailed *t*-test, $*P < 0.05$). **l**, Quantitative RT-PCR analysis of the percentage relative expression of *opn1lw1*, *gnb3a* and *crx* in adult wild-type sibling (orange columns) and *dnmt3bb.1*²⁵⁸ mutant (blue columns) zebrafish eyes, normalized to wild-type sibling levels. Data represent means \pm s.e.m. of three biological replicates (two-tailed *t*-test, $*P < 0.005$). **m**, Quantitative RT-PCR analysis of the percentage relative expression of *dnmt3bb.1* in surface and cave morphs of *A. mexicanus*, normalized to surface fish levels. Data represent means \pm s.e.m. of three biological replicates (two-tailed *t*-test, $*P < 0.05$). All images are lateral views, rostral to the left. Scale bars: 100 μ m in a and b; 250 μ m in c and d; 3 mm in e and f; 50 μ m in h; 1 mm in i and j.

fish eyes at 54 h post-fertilization, during a critical period for eye development in Pachón cavefish¹⁰ (Fig. 2a). RNA-Seq analysis confirmed increased expression of *dnmt3bb.1* in cavefish eyes (Fig. 2b,c). The RNA-Seq data also revealed that a large number of different eye development genes show reduced expression in cavefish eyes (Fig. 2c and Supplementary Data 1). As in the naked mole rat, visual perception (GO:0007601) and electrophysiology of the eye are the top downregulated biological processes found using Gene Ontology (Fig. 2d) and Ingenuity Pathway Analysis (Supplementary Fig. 3), respectively. Ingenuity Pathway Analysis also predicted that the phototransduction pathway is the most affected signalling pathway in cavefish eyes compared with surface fish eyes (Supplementary Fig. 3).

Previous studies have shown that promoter methylation is highly correlated with gene repression¹⁷. In total, 128 genes show substantially increased methylation within the 2 kilobases of genomic DNA upstream from the transcriptional start site in cavefish versus surface fish ($\geq 15\%$ increase; $P \leq 0.05$) and decreased expression in cavefish eyes compared with surface fish eyes (fold decrease ≤ 1.5 ; $P \leq 0.05$) (Supplementary Data 2). These include 39 and 26 genes annotated as having eye expression in mice and humans, respectively (Supplementary Data 3). Interestingly, 19 of these genes have been previously linked to human eye disorders (Table 1). These include *opn1lw1*, an opsin associated with cone-rod dystrophy and colourblindness^{18,19}, *gnb3a*, which is defective in autosomal recessive congenital stationary night blindness^{20,21}, and *crx*, a photoreceptor-specific transcription factor whose loss leads to blindness in humans^{22,23}. Targeted bisulfite sequencing of DNA amplified from the *opn1lw1*, *gnb3a* and *crx* promoter regions from surface fish or cavefish eyes at 54 h post-fertilization confirms increased methylation of CpGs in the 5' upstream sequences of each of these three genes (Fig. 2e,g,i,k,m,o and Supplementary Fig. 4). Whole-mount in situ hybridization using *opn1lw1*, *gnb3a* and *crx* probes also strongly verifies decreased expression of the three genes in cavefish versus surface fish eyes (Fig. 2f,h,j,l,n,p). Together, these data show that the expression of key human-eye-disease-associated eye development genes is reduced in Pachón cavefish compared with their surface fish relatives, and that many of these eye genes also display increased promoter methylation. Interestingly, the *crx* transcription factor is itself necessary for proper expression of a large number of additional eye genes²³, many of which are also strongly reduced in cavefish eyes, even though most of these genes are not themselves methylated (Supplementary Fig. 5).

Increased expression of eye genes, such as *opn1lw1*, *gnb3a* and *crx* (Fig. 1l), and increased eye size (Fig. 1m) in *dnmt3bb.1* mutant zebrafish is consistent with the hypothesis that DNA methylation represses eye gene expression to restrain or limit eye development. To test this idea experimentally, we examined whether increasing DNA methylation levels results in decreased eye gene expression and reduced eye development, using previously described zebrafish *ten-eleven translocation methylcytosine dioxygenase* (*TET*) mutants that display global DNA hypermethylation²⁴. Unlike DNMTs, which add methyl groups to cytosines to generate 5-methylcytosine, TET proteins oxidize methylcytosine to hydroxyl-methylcytosine, promoting DNA demethylation^{25,26}. Like mammals, zebrafish have three TET enzymes with partially redundant functions: Tet1, Tet2 and Tet3. Tet2 and Tet3 are the main TET proteins responsible for converting methylcytosine into hydroxymethylcytosine; zebrafish *tet1*^{-/-}, *tet2*^{-/-}, *tet3*^{-/-} triple mutants do not show additional phenotypes compared with *tet2*^{-/-}, *tet3*^{-/-} double mutants²⁴. We found that *tet2*^{-/-}, *tet3*^{-/-} double mutants have smaller eyes than their wild-type siblings (Fig. 3a–c). Targeted bisulfite sequencing and quantitative PCR with reverse transcription (RT-PCR) on nucleic acids from whole eyes dissected from *tet2*^{-/-}, *tet3*^{-/-} double mutants and their wild-type siblings at 48 h post-fertilization also revealed increased

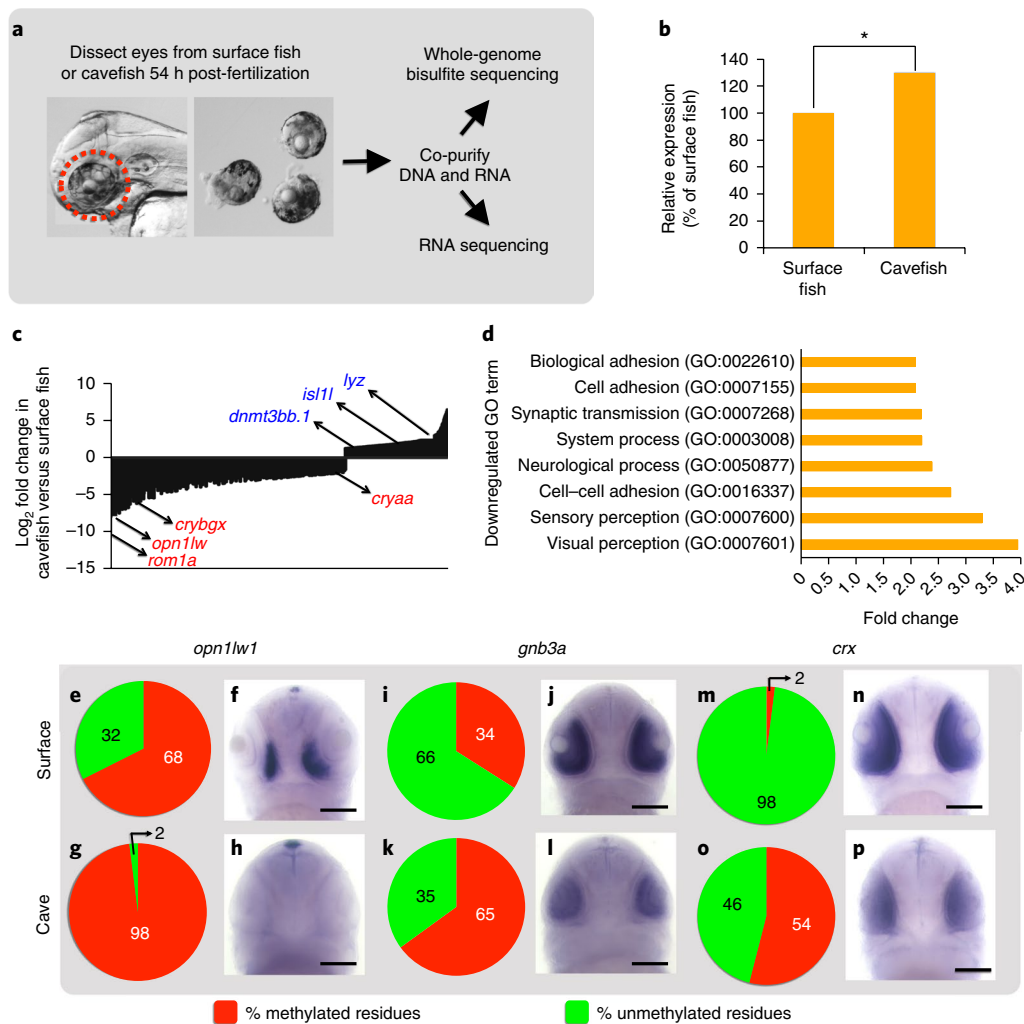


Fig. 2 | Gene expression changes in cave versus surface fish morphs of *A. mexicanus*. **a**, Workflow for obtaining larval eyes from *A. mexicanus* and co-isolating eye DNA and RNA for whole-genome assessment of DNA methylation and gene expression, respectively. **b**, Percentage relative expression (fragments per kilobase of transcript per million mapped reads) of *dnmt3bb.1* in the eyes of *A. mexicanus* cave versus surface fish morphs by comparison of their respective RNA-Seq datasets (two replicates), normalized to surface fish levels (* $P < 0.05$). **c**, Log₂ fold differential expression ($P < 0.05$) of genes in *A. mexicanus* cave versus surface fish morph RNA-Seq datasets, with downregulated (red) or upregulated (blue) expression of selected genes in cavefish. **d**, Listing of the Gene Ontology (GO) terms showing the greatest downregulation in cavefish compared with surface fish. **e–p**, Assessment of *opn1lw1* (e–h), *gnb3a* (i–l) and *crx* (m–p) promoter DNA methylation (e, g, i, k, m and o) and gene expression (f, h, j, l, n and p) in surface (e, f, i, j, m and n) and cave (g, h, k, l, o and p) morphs of *A. mexicanus* at 54 h post-fertilization. Pie charts (e, g, i, k, m and o) show the percentage methylation of the promoter CpG. Images (f, h, j, l, n and p) show representative whole-mount in situ hybridization of the larval heads using *opn1lw1*, *gnb3a* and *crx* probes (ventral views, rostral up; a minimum of 20–25 embryos were analysed by in situ hybridization). Scale bars: 100 μ m.

crx and *gnb3a* promoter methylation (Fig. 3d–g and Supplementary Fig. 6) and reduced *crx* and *gnb3a* gene expression (Fig. 3h) in the double mutants. Like *dnmt3bb.1* mutants, *tet2*^{−/−}, *tet3*^{−/−} double mutants also show haematopoietic defects. In addition, after 48 h post-fertilization, *tet2*^{−/−}, *tet3*^{−/−} double mutants begin to deteriorate with defects in brain development, and do not survive beyond 5 days post-fertilization. These additional phenotypes may arise as a result of global DNA hypermethylation in these mutants.

To further test whether excess DNA methylation contributes to failure to maintain eye development in Pachón cavefish, we examined whether eye loss could be 'rescued' by pharmacological inhibition of DNA methylation. 5-Azacytidine (Aza) is a well-characterized inhibitor of DNA methylation²⁷ approved for the treatment of aberrant DNA methylation in patients with myelodysplastic syndrome²⁸. Since systemic administration of Aza to zebrafish embryos leads to severe pleiotropic defects and early lethality²⁹, we carried

out single injections of either Aza or control dimethylsulfoxide (DMSO) carrier into the vitreous chamber of the left eye of cavefish embryos at 42–48 h post-fertilization, and then scored phenotypes in both injected left and control right eyes at 5 days post-fertilization (Fig. 4a). A single early injection of Aza into the left eye resulted in larger eyes than either the control uninjected right eyes in the same animals or the DMSO-injected left eyes of other animals (Fig. 4b). Histological analysis confirmed that Aza-injected cavefish eyes at 5 days post-fertilization are significantly larger than uninjected or DMSO-injected controls, and that they possess a more organized structure including morphologically well-defined lens and retinal layers (Fig. 4c–e). Targeted promoter bisulfite sequencing of *gnb3a* from Aza-injected cavefish eyes revealed reduced DNA methylation at this locus (Supplementary Fig. 7a). Increased expression of *gnb3a* and *crx* was also noted in cavefish eyes injected with either Aza or the more 'DNA specific' drug 5-Aza-2'-deoxycytidine (Supplementary

Table 1 | Cavefish genes with significant promoter hypermethylation and reduced expression are associated with human eye disorders

Eye gene	Log ₂ fold change in gene expression	Change in promoter methylation (%)	Associated human eye disease
<i>STX3</i>	-2.65	15.05	Microvillus inclusion disease
<i>IMPG1</i>	-2.06	15.72	Macular dystrophy
<i>GNB3</i>	-2.15	15.75	Congenital night blindness
<i>RS1</i>	-4.81	16.22	Retinoschisis
<i>ELOVL4</i>	-2.73	16.92	Stargardt disease
<i>TRPM1</i>	-1.51	17.11	Congenital night blindness
<i>KCNV2</i>	-2.61	19.27	Retinal cone dystrophy
<i>HEPACAM</i>	-1.29	19.28	Macrocephaly
<i>CRX</i>	-1.34	20.36	Retinitis pigmentosa
<i>PDE6H</i>	-2.43	20.84	Retinal cone dystrophy
<i>PRPH2</i>	-4.61	21.92	Retinitis pigmentosa
<i>TMEM98</i>	-1.30	23.68	Nanophthalmia
<i>GRK1</i>	-4.39	24.78	Oguchi disease
<i>MYO7A</i>	-1.34	31.20	Usher syndrome
<i>ATP6V0A1</i>	-1.46	32.70	Macroautophagy
<i>TDRD7</i>	-1.82	34.98	Cataract
<i>OPN1MW</i>	-7.26	36.78	Cone-rod dystrophy
<i>CRYGB</i>	-4.13	39.28	Polar cataract
<i>OPN1LW</i>	-4.15	47.98	Cone-rod dystrophy

Fig. 7b), suggesting that inhibiting the excess methylation of eye genes in cavefish results in increased expression of these genes and at least a partial 'rescue' of eye development.

Together, our results suggest that DNA methylation plays a critical role in teleost eye development, and that increased DNA methylation-based eye gene repression is a major molecular mechanism underlying cavefish eye degeneration (Fig. 4f). Many of the key eye genes downregulated in cavefish are conserved in humans and linked to eye disease and/or blindness, suggesting a potential conserved function for these genes across evolution. Although a central role for DNA methylation in development and disease has been well documented^{30,31}, our results suggest that small genetic changes that alter epigenetic regulation can play an important role in rapid adaptive evolution by triggering dramatic changes in the expression of large sets of genes. There is precedent for epigenetic changes resulting in dramatically altered developmental fates; for example, nutrition-driven changes in DNA methylation regulate the switch between queen and worker caste specification in honeybees (*Apis mellifera*)³². Our findings indicate that eye loss in Pachón cavefish occurs via distinct molecular mechanisms compared with naked mole rats, where inactivating mutations are found in multiple key eye genes. This could reflect differences in their evolutionary timescales. Cavefish evolved over the past one to five million years¹, while naked mole rats evolved 73 million years ago⁸, allowing sufficient time to fix and select acquired mutations in genes essential for eye development. It remains to be seen whether altered epigenetic regulation has been used to generate phenotypic variability in other rapidly evolved animals.

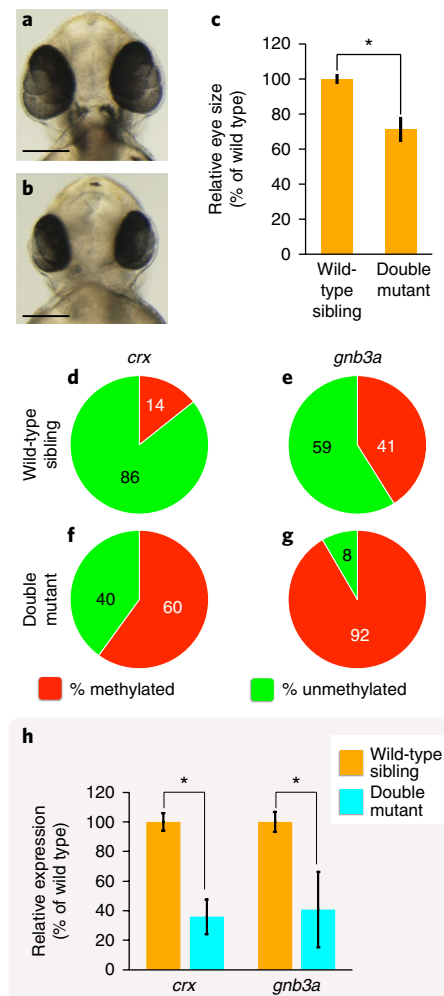


Fig. 3 | Eye phenotype and associated gene expression changes in wild-type and DNA methylation-deficient *D. rerio*. **a, b**, Transmitted light photomicrographs of the heads of wild-type sibling (**a**) and *tet2*^{-/-}, *tet3*^{-/-} double-mutant embryos (**b**) at 48 h post-fertilization. Scale bars: 100 μ M. **c**, Quantitation of eye size in wild-type sibling and *tet2*^{-/-}, *tet3*^{-/-} double-mutant embryos at 48 h post-fertilization. Data represent means \pm s.d. ($n=10$) (two-tailed *t*-test, * $P < 0.05$). **d–g**, Assessment of *crx* (**d** and **f**) and *gnb3a* (**e** and **g**) promoter DNA methylation in isolated eyes from wild-type sibling (**d** and **e**) and *tet2*^{-/-}, *tet3*^{-/-} double-mutant embryos (**f** and **g**) at 48 h post-fertilization. **h**, Quantitative RT-PCR analysis of the percentage relative expression of *crx* and *gnb3a* in isolated eyes from wild-type sibling (orange columns) and *tet2*^{-/-}, *tet3*^{-/-} double-mutant embryos (blue columns) at 48 h post-fertilization. Data represent means \pm s.e.m. of three biological replicates (two-tailed *t*-test, * $P < 0.005$).

Methods

Fish stocks and embryos. The zebrafish lines used in this study include *dnmt3bb*.1y²⁵⁸ (ref. 13) and *tet2*^{mk17}, *tet3*^{mk18} (ref. 24) mutants, as well as the EkkWill wild-type line. Surface and Pachón cave populations of *A. mexicanus* were also used. Fish were spawned naturally and embryos were raised and staged as described previously^{33,34}. All of the animals were handled according to approved Institutional Animal Care and Use Committee protocols (12-039 and 18-016) of the National Institute of Child Health and Human Development.

Genomic DNA isolation, bisulfite conversion and sequencing. Surface fish and cavefish embryos were raised to the stages described. Dechorionated embryos were transferred into 1 \times phosphate buffered saline without calcium and magnesium. Eyes were surgically removed using a pair of fine-tip tungsten needles. Total cellular RNA and DNA was isolated from harvested eyes using an ZR-Duet DNA/RNA MiniPrep Kit (Zymo Research). For whole-genome bisulfite sequencing, 200 ng of purified genomic DNA was bisulfite converted using an EZ

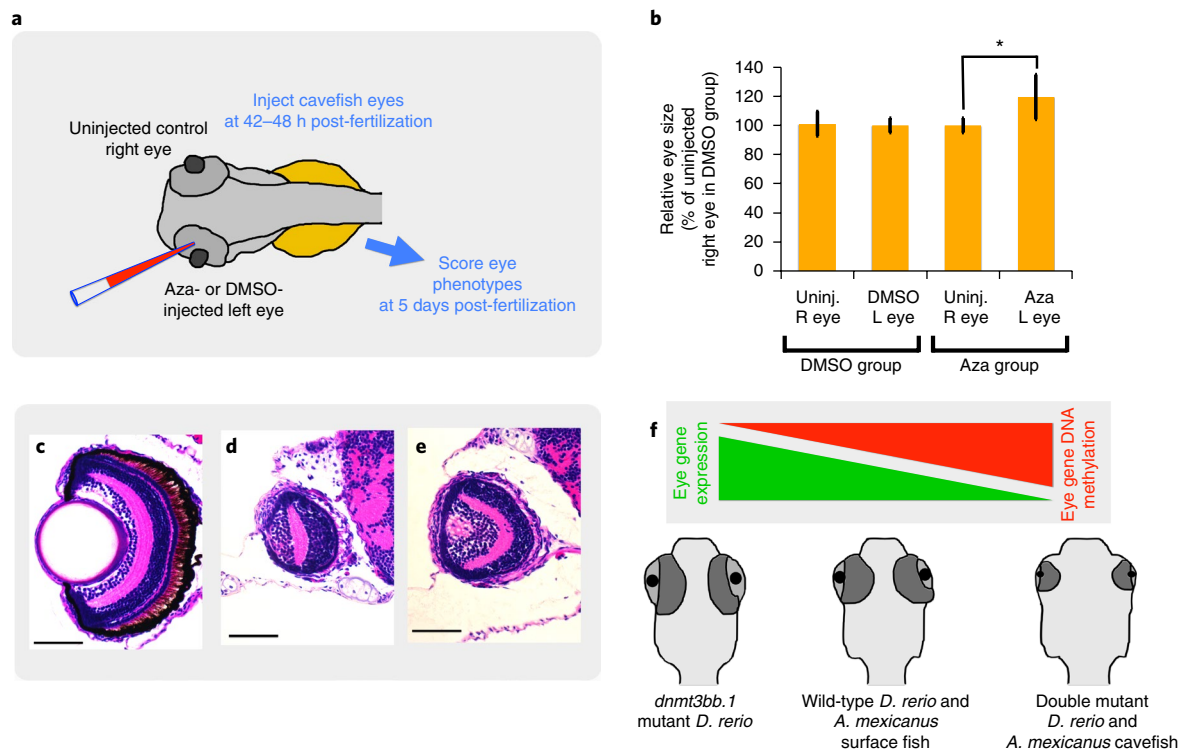


Fig. 4 | Partial rescue of cavefish eyes by Aza-mediated inhibition of eye DNA methylation. **a**, Schematic showing the experimental procedure for injection of DMSO or Aza into cavefish embryo eyes at 42–48 h post-fertilization. **b**, Quantitation of eye size in *A. mexicanus* embryos at 5 days post-fertilization that were injected in the left (L) eye with DMSO or Aza. Data represent means \pm s.d. (DMSO group, $n = 18$; Aza group, $n = 12$) (two-tailed t -test, $*P < 0.05$). R, right; Uninj., uninjected. **c–e**, Representative histological analysis of the eyes of a haematoxylin-and-eosin-stained surface fish (**c**), DMSO-injected cavefish (**d**) and Aza-injected cavefish (**e**) at 5 days post-fertilization (four to eight embryos per condition were sectioned and analysed). Scale bars: 100 μ m. **f**, Model depicting the role of DNA methylation in teleost eye development and degeneration. Hypermethylation and downregulation of eye gene expression in cavefish and zebrafish $tet^{2/3}$ double mutants leads to eye degeneration.

DNA Methylation-Lightning kit (Zymo Research). Next-generation sequencing libraries were generated from the bisulfite-converted DNA using a TruSeq DNA Methylation Kit and TruSeq DNA Methylation Index PCR Primers (Illumina). Sequencing libraries of two biological replicates from surface fish and cavefish were run separately on two flow cells of an Illumina HiSeq 2500 sequencer operated in the rapid run mode with V2 chemistry to yield about 400 million read-pair reads (2×100 base pairs (bp)) for each sample. Raw single-end sequence data were trimmed for quality and adaptor sequence using Trimmomatic software³⁵, trimming leading or trailing bases at a quality of <5 , as well as using a sliding window requiring a 4-bp average with a quality of >15 . Reads trimmed below 50 bp were discarded. Following trimming, reads were aligned using Bismark software³⁶ against a bisulfite-converted Pachón cavefish genome using non-directional alignment. Using defined gene coordinates, gene body and promoter regions 2 kilobases upstream from the transcriptional start site were assigned, and combined conversions and non-conversions were summed to provide an overall bisulfite conversion rate per region. The ratio of conversions was then tested for change between conditions, using a two-proportion z -test to test the hypothesis that the proportion of bisulfite conversion had altered between the conditions. For targeted bisulfite analysis, bisulfite-converted DNA was PCR amplified using primers designed by MethPrimer³⁷ (<http://www.urogene.org/cgi-bin/methprimer/methprimer.cgi>). OneTaq Hot Start 2X Master Mix in DNA polymerase with standard buffer (NEB) was used to amplify the bisulfite-converted DNA. PCR amplicons were purified and cloned using a pCRII-TOPO TA Cloning Kit (Thermo Fisher Scientific). MiniPrep plasmid DNA was sequenced using T7 or SP6 sequencing primers. The sequencing results were analysed using QUMA³⁸ (<http://quma.cdb.riken.jp/>).

RNA isolation and sequencing. Total cellular RNA and DNA was isolated from the harvested eyes using the ZR-Duet DNA/RNA MiniPrep Kit (Zymo Research). Some 300–900 ng of poly-A-enriched RNA was converted to indexed sequencing libraries using a TruSeq Standard mRNA Library Prep Kit (Illumina). Libraries for two biological replicates of surface fish and cavefish were combined and run on one flow cell of an Illumina HiSeq 2500 sequencer in rapid run mode with V2 chemistry. We sequenced 100 million paired-end reads per sample. Paired-end reads were trimmed using Trimmomatic and aligned to the Pachón cavefish genome using RNA-STAR. Quantitation was performed with subread feature

counts and differential expression analysis was performed with count data via DESeq2. Human, mouse and zebrafish homologues of cavefish genes were identified using Ensembl BioMart. Ingenuity Pathway Analysis and PANTHER Gene Ontology term-enrichment analysis were carried out on RNA-Seq data to identify the major signalling pathways and networks affected based on differentially expressed genes.

RNA isolation, complementary DNA synthesis and quantitative RT-PCR. Total cellular RNA was isolated from harvested eyes and other tissues as mentioned above, using the ZR-Duet DNA/RNA MiniPrep Kit (Zymo Research). Equal amounts of RNA were converted into complementary DNA using a ThermoScript RT-PCR System (Invitrogen). Resulting complementary DNA was used in quantitative PCR using SsoAdvanced Universal SYBR Green Supermix (Bio-Rad) on a CFX96 Real-Time system. A minimum of three biological replicates were performed. The primers used in this study are listed in Supplementary Data 4.

Riboprobe synthesis, in situ hybridization and histology. Antisense riboprobes were generated using Roche DIG and FITC Labeling Mix. Portions of the coding regions of genes were PCR amplified using OneTaq Hot Start 2X Master Mix in DNA polymerase with standard buffer (NEB) and cloned into pCRII-TOPO TA vector (Thermo Fisher Scientific). Sequence-verified clones were used to generate antisense riboprobes using the appropriate enzymes. The zebrafish *dnmt3bb.1* probe was generated as described previously¹³. Whole-mount in situ hybridization was carried out as described previously with a few modifications. To reduce non-specific hybridization and enhance the signal-to-noise ratio, we used 5% dextran sulfate (Sigma–Aldrich) in the hybridization buffer and pre-adsorbed anti-DIG and anti-FITC antibodies to whole cavefish powder. For histology, embryos and tissue samples were fixed using 4% paraformaldehyde overnight at 4°C and subsequently passed through ascending grades of alcohol followed by paraffin embedding. Sections were stained with haematoxylin and eosin.

Microinjection. Microinjection of 5-Azacytidine or 5-Aza-2'-deoxycytidine (Sigma–Aldrich) into Pachón cavefish embryonic eyes was carried out in embryos at 42–48 h post-fertilization. Embryos were mounted laterally in low-melting-point agarose. Injection needles were pulled from filament-containing glass capillaries (World Precision Instruments; catalogue number TW100F-4) using a

needle puller (Sutter Instrument). Needles were back-loaded and a single 1–2 nl bolus of either 100 μ M 5-Azacytidine or 5-Aza-2'-deoxycytidine in 5% DMSO or 5% DMSO carrier alone was delivered into the vitreous of the left eye using a Pneumatic PicoPump (World Precision Instruments). Embryos were removed from the agarose, allowed to continue to develop until 5 days post-fertilization, and then scored for eye size and/or used for histological analysis of the eyes. Injected embryos with axis or brain deformities were discarded from the analysis.

Eye size quantifications. For the eye size measurements, mutant, treated and control embryos were imaged at the same magnification. All eye size measurements were performed by normalizing the area of the eyes to the head. A Student's *t*-test (paired) was performed on the normalized eye sizes.

Reporting Summary. Further information on experimental design is available in the Nature Research Reporting Summary linked to this article.

Data availability. Sequencing data have been deposited in the Gene Expression Omnibus database under accession number GSE109006.

Received: 17 December 2017; Accepted: 2 May 2018;

Published online: 28 May 2018

References

- Gross, J. B., Meyer, B. & Perkins, M. The rise of *Astyanax* cavefish. *Dev. Dynam.* **244**, 1031–1038 (2015).
- Moran, D., Softley, R. & Warrant, E. J. The energetic cost of vision and the evolution of eyeless Mexican cavefish. *Sci. Adv.* **1**, e1500363 (2015).
- Hinaux, H. et al. Lens defects in *Astyanax mexicanus* cavefish: evolution of crystallins and a role for alphaA-crystallin. *Dev. Neurobiol.* **75**, 505–521 (2015).
- Casane, D. & Retaux, S. Evolutionary genetics of the cavefish *Astyanax mexicanus*. *Adv. Genet.* **95**, 117–159 (2016).
- Ma, L., Parkhurst, A. & Jeffery, W. R. The role of a lens survival pathway including *sox2* and *alphaA-crystallin* in the evolution of cavefish eye degeneration. *EvoDevo* **5**, 28 (2014).
- McGaugh, S. E. et al. The cavefish genome reveals candidate genes for eye loss. *Nat. Commun.* **5**, 5307 (2014).
- Hinaux, H. et al. De novo sequencing of *Astyanax mexicanus* surface fish and Pachón cavefish transcriptomes reveals enrichment of mutations in cavefish putative eye genes. *PLoS ONE* **8**, e53553 (2013).
- Kim, E. B. et al. Genome sequencing reveals insights into physiology and longevity of the naked mole rat. *Nature* **479**, 223–227 (2011).
- Zhu, H., Wang, G. & Qian, J. Transcription factors as readers and effectors of DNA methylation. *Nat. Rev. Genet.* **17**, 551–565 (2016).
- Strickler, A. G., Yamamoto, Y. & Jeffery, W. R. The lens controls cell survival in the retina: evidence from the blind cavefish *Astyanax*. *Dev. Biol.* **311**, 512–523 (2007).
- Csankovszki, G., Nagy, A. & Jaenisch, R. Synergism of Xist RNA, DNA methylation, and histone hypoacetylation in maintaining X chromosome inactivation. *J. Cell Biol.* **153**, 773–784 (2001).
- Xu, F. et al. Molecular and enzymatic profiles of mammalian DNA methyltransferases: structures and targets for drugs. *Curr. Med. Chem.* **17**, 4052–4071 (2010).
- Gore, A. V. et al. Epigenetic regulation of hematopoiesis by DNA methylation. *eLife* **5**, e11813 (2016).
- Seritkul, P. & Gross, J. M. Expression of the de novo DNA methyltransferases (*dnmt3–dnmt8*) during zebrafish lens development. *Dev. Dynam.* **243**, 350–356 (2014).
- Raymond, P. A., Barthel, L. K., Bernardos, R. L. & Perkowski, J. J. Molecular characterization of retinal stem cells and their niches in adult zebrafish. *BMC Dev. Biol.* **6**, 36 (2006).
- Wan, Y. et al. The ciliary marginal zone of the zebrafish retina: clonal and time-lapse analysis of a continuously growing tissue. *Development* **143**, 1099–1107 (2016).
- Stirzaker, C., Taberlay, P. C., Statham, A. L. & Clark, S. J. Mining cancer methylomes: prospects and challenges. *Trends Genet.* **30**, 75–84 (2014).
- Ayyagari, R. et al. Bilateral macular atrophy in blue cone monochromacy (BCM) with loss of the locus control region (LCR) and part of the red pigment gene. *Mol. Vis.* **5**, 13 (1999).
- Winderickx, J. et al. Defective colour vision associated with a missense mutation in the human green visual pigment gene. *Nat. Genet.* **1**, 251–256 (1992).
- Arno, G. et al. Recessive retinopathy consequent on mutant G-protein β subunit 3 (*GNB3*). *JAMA Ophthalmol.* **134**, 924–927 (2016).
- Vincent, A. et al. Biallelic mutations in *GNB3* cause a unique form of autosomal-recessive congenital stationary night blindness. *Am. J. Hum. Genet.* **98**, 1011–1019 (2016).
- Swaroop, A. et al. Leber congenital amaurosis caused by a homozygous mutation (*R90W*) in the homeodomain of the retinal transcription factor CRX: direct evidence for the involvement of CRX in the development of photoreceptor function. *Hum. Mol. Genet.* **8**, 299–305 (1999).
- Swaroop, A., Kim, D. & Forrest, D. Transcriptional regulation of photoreceptor development and homeostasis in the mammalian retina. *Nat. Rev. Neurosci.* **11**, 563–576 (2010).
- Li, C. et al. Overlapping requirements for Tet2 and Tet3 in normal development and hematopoietic stem cell emergence. *Cell Rep.* **12**, 1133–1143 (2015).
- Ito, S. et al. Role of Tet proteins in 5mC to 5hmC conversion, ES-cell self-renewal and inner cell mass specification. *Nature* **466**, 1129–1133 (2010).
- Ito, S. et al. Tet proteins can convert 5-methylcytosine to 5-formylcytosine and 5-carboxylcytosine. *Science* **333**, 1300–1303 (2011).
- Jones, P. A. & Taylor, S. M. Cellular differentiation, cytidine analogs and DNA methylation. *Cell* **20**, 85–93 (1980).
- Raj, K. & Mufti, G. J. Azacytidine (Vidaza®) in the treatment of myelodysplastic syndromes. *Ther. Clin. Risk Manag.* **2**, 377–388 (2006).
- Martin, C. C., Laforest, L., Akimenko, M. A. & Ekker, M. A role for DNA methylation in gastrulation and somite patterning. *Dev. Biol.* **206**, 189–205 (1999).
- Heyn, H. & Esteller, M. DNA methylation profiling in the clinic: applications and challenges. *Nat. Rev. Genet.* **13**, 679–692 (2012).
- Suzuki, M. M. & Bird, A. DNA methylation landscapes: provocative insights from epigenomics. *Nat. Rev. Genet.* **9**, 465–476 (2008).
- Kucharski, R., Maleszka, J., Foret, S. & Maleszka, R. Nutritional control of reproductive status in honeybees via DNA methylation. *Science* **319**, 1827–1830 (2008).
- Kimmel, C. B., Ballard, W. W., Kimmel, S. R., Ullmann, B. & Schilling, T. F. Stages of embryonic development of the zebrafish. *Dev. Dyn.* **203**, 253–310 (1995).
- Elipot, Y., Legendre, L., Pere, S., Sohm, F. & Retaux, S. *Astyanax* transgenesis and husbandry: how cavefish enters the laboratory. *Zebrafish* **11**, 291–299 (2014).
- Bolger, A. M., Lohse, M., & Usadel, B. Trimmomatic: a flexible trimmer for Illumina sequence data. *Bioinformatics* **30**, 2114–2120 (2014).
- Krueger, F., Andrews, S. R. Bismark: a flexible aligner and methylation caller for Bisulfite-Seq applications. *Bioinformatics* **27**, 1571–1572 (2011).
- Li, L. C. & Dahiya, R. MethPrimer: designing primers for methylation PCRs. *Bioinformatics* **18**, 1427–1431 (2002).
- Kumaki, Y., Oda, M. & Okano, M. QUMA: quantification tool for methylation analysis. *Nucleic Acids Res.* **36**, W170–W175 (2008).

Acknowledgements

We thank members of the Weinstein and Jeffery laboratories for support, help and suggestions. We thank staff at the NICHD's Molecular Genomics Laboratory for bisulfite and RNA-Seq assistance. We also thank members of the zebrafish and cavefish communities for sharing reagents and protocols. We thank K. Sampath for comments on the manuscript. We thank S. McGaugh for suggestions on cavefish sequence alignments and M. Goll for providing the zebrafish *tet2,3* double mutant line. Work in the Weinstein and Jeffery laboratories is supported by the intramural programme of the NICHD and by R01EY024941, respectively.

Author contributions

A.V.G. and B.M.W. designed the study with input from K.A.T. and W.R.J. A.V.G. and K.A.T. performed the experiments with help from L.M., D.C. and A.E.D. J.I. analysed the sequencing data. D.C. and A.E.D. provided fish husbandry support. A.V.G. and B.M.W. wrote the manuscript with input from all authors.

Competing interests

The authors declare no competing interests.

Additional information

Supplementary information is available for this paper at <https://doi.org/10.1038/s41559-018-0569-4>.

Reprints and permissions information is available at www.nature.com/reprints.

Correspondence and requests for materials should be addressed to A.V.G. or B.M.W.

Publisher's note: Springer Nature remains neutral with regard to jurisdictional claims in published maps and institutional affiliations.

Life Sciences Reporting Summary

Nature Research wishes to improve the reproducibility of the work that we publish. This form is intended for publication with all accepted life science papers and provides structure for consistency and transparency in reporting. Every life science submission will use this form; some list items might not apply to an individual manuscript, but all fields must be completed for clarity.

For further information on the points included in this form, see [Reporting Life Sciences Research](#). For further information on Nature Research policies, including our [data availability policy](#), see [Authors & Referees](#) and the [Editorial Policy Checklist](#).

Please do not complete any field with "not applicable" or n/a. Refer to the help text for what text to use if an item is not relevant to your study. [For final submission](#): please carefully check your responses for accuracy; you will not be able to make changes later.

► Experimental design

1. Sample size

Describe how sample size was determined.

Whole genome bisulfite and RNA seq sample sizes were determined based on previous published literature and biostatistician's recommendation.

2. Data exclusions

Describe any data exclusions.

We excluded non-viable and abnormally developed embryos from our analyses.

3. Replication

Describe the measures taken to verify the reproducibility of the experimental findings.

Two biological replicates were performed for RNA seq. For RT-qPCRs, at least three biological replicates were performed to confirm the consistency and successful reproduction of the results.

4. Randomization

Describe how samples/organisms/participants were allocated into experimental groups.

After selecting surviving embryos, controls, mutants and treated animals were scored as described in methods section and figure legends.

5. Blinding

Describe whether the investigators were blinded to group allocation during data collection and/or analysis.

Authors were not blinded because of the obvious morphological phenotypes. Authors were aware of the embryos injected with control DMSO or Aza or AzaD. Quantitative measurements were performed to verify subjectively observed results.

Note: all in vivo studies must report how sample size was determined and whether blinding and randomization were used.

6. Statistical parameters

For all figures and tables that use statistical methods, confirm that the following items are present in relevant figure legends (or in the Methods section if additional space is needed).

n/a Confirmed

- ☐ ☒ The exact sample size (*n*) for each experimental group/condition, given as a discrete number and unit of measurement (animals, litters, cultures, etc.)
- ☐ ☒ A description of how samples were collected, noting whether measurements were taken from distinct samples or whether the same sample was measured repeatedly
- ☐ ☒ A statement indicating how many times each experiment was replicated
- ☐ ☒ The statistical test(s) used and whether they are one- or two-sided
Only common tests should be described solely by name; describe more complex techniques in the Methods section.
- ☒ ☐ A description of any assumptions or corrections, such as an adjustment for multiple comparisons
- ☐ ☒ Test values indicating whether an effect is present
*Provide confidence intervals or give results of significance tests (e.g. *P* values) as exact values whenever appropriate and with effect sizes noted.*
- ☐ ☒ A clear description of statistics including central tendency (e.g. median, mean) and variation (e.g. standard deviation, interquartile range)
- ☐ ☒ Clearly defined error bars in all relevant figure captions (with explicit mention of central tendency and variation)

See the web collection on [statistics for biologists](#) for further resources and guidance.

► Software

Policy information about [availability of computer code](#)

7. Software

Describe the software used to analyze the data in this study.

Trimmomatic, Bismark, RNA-STAR, DESeq2, Microsoft Excel, Microsoft Powerpoint, and Photoshop.

For manuscripts utilizing custom algorithms or software that are central to the paper but not yet described in the published literature, software must be made available to editors and reviewers upon request. We strongly encourage code deposition in a community repository (e.g. GitHub). *Nature Methods* [guidance for providing algorithms and software for publication](#) provides further information on this topic.

► Materials and reagents

Policy information about [availability of materials](#)

8. Materials availability

Indicate whether there are restrictions on availability of unique materials or if these materials are only available for distribution by a third party.

No unique materials were used.

9. Antibodies

Describe the antibodies used and how they were validated for use in the system under study (i.e. assay and species).

Sheep Anti-Digoxigenin-AP (11 093 274 910) Roche used for developing in situ hybridization stainings, validated in Thisse and Thisse, 2008 Nat. Protoc.

10. Eukaryotic cell lines

a. State the source of each eukaryotic cell line used.

No eukaryotic cell lines were used in this study.

b. Describe the method of cell line authentication used.

No eukaryotic cell lines were used in this study.

c. Report whether the cell lines were tested for mycoplasma contamination.

No eukaryotic cell lines were used in this study.

d. If any of the cell lines used are listed in the database of commonly misidentified cell lines maintained by [ICLAC](#), provide a scientific rationale for their use.

No eukaryotic cell lines were used in this study.

► Animals and human research participants

Policy information about [studies involving animals](#); when reporting animal research, follow the [ARRIVE guidelines](#)

11. Description of research animals

Provide all relevant details on animals and/or animal-derived materials used in the study.

Adult Zebrafish (*Danio rerio*) and *Astyanax mexicanus* were used to obtain embryos by natural matings. Embryos and larvae up to day 5 were used in different analyses.

Policy information about [studies involving human research participants](#)

12. Description of human research participants

Describe the covariate-relevant population characteristics of the human research participants.

This study did not involve the use of human research participants